특별강연 I

막기공에서의 용질분배와 배제에 대한 콜로이드 상호작용의 역할

전 명 석

한국과학기술연구원 高分子部 分離膜室

The Role of Colloidal Interactions on the Solute Partitioning and the Rejection Occurred in Membrane Pores

Myung-Suk Chun

Membranes Lab (Phone: 958-5363), Polymers Division, KIST, Seoul 130-650

A rigorous analysis on the effect of colloidal interactions on the separation characteristic has been extended to the case of *non-dilute* charged solute concentration. The solute partitioning within slit pores for a wide range of solute concentration has been predicted by performing the *Monte Carlo technique*. Using a hindered transport model, rejection coefficients have been estimated from the predicted concentration profile.

Introduction

The interest on the behavior of hydrodynamic colloidal particles within the narrow spaces is needed to develop a number of related membrane separation processes such as ultrafiltration and microfiltration [1,2]. Long ago, it has been proved that *long-range electrostatic interactions* [3] between the particles and the adjacent solid surfaces play a major ingredient in the physicochemical problems of aqueous colloidal suspensions. The diversity of such problems may be illustrated readily by a few situations: the modification of concentration profile in the microcapillary column and the velocity enhancement in capillary flows of water-soluble polymers [4,5].

It is obvious that efforts to elucidate the membrane separation properties have been almost confined to the case of infinitely dilute solute concentration, however, the solute concentration in real situations of membrane filtration is non-dilute. For non-dilute solute concentrations, or when the pores of interest have geometries more complicated, modeling partitioning and rejection behavior by using virial expansions or density functional theory is fairly difficult. In this work, by employing the numerical approach based on the *Gibbs ensemble Monte Carlo* (GEMC) technique, evaluations of the concentration profile in the membrane pore have been performed for both charged and uncharged systems for a wide range of solute concentration.

The Principles and Model Developments

Concentration partitioning of charged colloidal particles is an important aspect of hindered diffusion or solute transport [6,7], besides a number of related molecular separations. The *partition coefficient* K, defined as the ratio of mean pore-to-bulk concentration, can be expressed as

$$K = \frac{C_{pore}}{C_{\infty}} = \frac{\int\int d\xi \; d\Omega \exp(-E/kT)}{\int\int d\xi \; d\Omega} \qquad (1)$$

where E/kT is the potential energy function of electrostatic interaction, and ξ and Ω are coordinate vectors describing particle position and orientation, respectively. Both wall-particle and particle-particle energy profiles are determined by using the recent analysis [8], that provides accurate solutions to the linearized Poisson-Boltzmann equation. This equation incorporated with a constant surface charge boundary condition can be solved by presenting a *singularity* method, which is similar to an approach applied in low Reynolds number hydrodynamics problem. The singularity strengths are found after a least-square regression for the unknown singularity. Once the force F on the sphere is known, the interaction energy may be obtained according to

$$E = \int_0^h F\, dz = \int_0^h \int_S \boldsymbol{T} \cdot \boldsymbol{n}\, dS\, dz \,. \tag{2}$$

Gibbs ensemble Monte Carlo (GEMC) method

In the GEMC method, the subsystems are allowed to interchange particles and the volumes allowed to fluctuate in order to satisfy the equilibrium conditions of the temperature, pressure, and chemical potential μ in each of the subsystems [9]. In essence, elements of canonical (NVT), isobaric-isothermal (NPT), and grand canonical (μVT) ensembles are combined in the Gibbs ensemble, so a computation cycle comprises three types of moves in this simulation. In our pore-bulk system, however, there are no attempted exchanges of volumes, as the condition for mechanical equilibrium is automatically satisfied if the chemical potentials in each regions are equal. Only two kinds of move with particle displacement and interchange are performed as shown in Fig.1. Figure 2 shows the location of surface points for a sphere. The accepting probabilities for the particle displacement (NVT Metropolis scheme) and interchange (from subsystem α to subsystem β) take the form, respectively, as

$$\mathbf{P}_D = \min\left[1,\ \exp\left(-\frac{\Delta E^{\alpha}}{kT}\right)\right] \tag{3}$$

$$\mathbf{P}_T = \min\left[1,\ \exp\left\{\ln\left(\frac{N^{\alpha}\, V^{\beta}}{(N^{\beta}+1)\, V^{\alpha}}\right) - \frac{\Delta E^{\alpha} + \Delta E^{\beta}}{kT}\right\}\right]. \tag{4}$$

A sufficiently large number of solute particles (usually 500~1300) is used so as to ensure that the results are independent of system size, and $2\sim4\times10^4$ configurations are required to reach equilibrium [8]. All of computations were carried out accurately on a Hewlett-Packard 9000 715/100 workstation (Palo Alto, CA).

It has been traditional to characterize the properties of a membrane filtration with respect to the solute transport in terms of membrane rejection. Basically, the rejection coefficient is said to have originated with a relationship between hindered transport principle and certain phenomenological transport coefficients (e.g., convective transport) for porous membranes [6,10]. With the flowing in Poiseuillean fashion, the resulting expression in terms of the retentate and the filtrate concentration is given by

$$\begin{aligned} R_j &= 1 - \frac{C_{filtrate}}{C_{feed}} \\ &= 1 - \frac{3/2}{C_o}\int_0^{1-\lambda} G(\lambda,\beta)(1-\beta^2)C(\beta)\,d\beta \end{aligned} \tag{5}$$

where the centerline approximation is applied for the solute lag coefficient G, and λ and β are the solute radius and radial coordinate, respectively, both normalized by the pore width. The $C(\beta)$ can be obtained by the curve-fit scheme on the predicted density profile.

Results

In Fig.3, GEMC results of uncharged systems are compared with the previous results. It can be seen that, for solute concentrations less than 10.9%, GEMC results are nearly identical to both those obtained by the virial expansion method and linear density functional theory for values of the ratio λ up to approximately 0.6. The presence of electrostatic interactions affects partitioning behavior. In the dilute limit, repulsion between the solute and pore walls leads to a sharp decrease in the partition coefficient, as shown in Fig.4. Ionic strengths range from 0.1 to 100mM, under which conditions the dimensionless, *inverse Debye lengths* κa vary from 0.656 to 20, respectively. As the double layer thickness increases, the importance of the repulsive interactions is enhanced. Figure 5 shows that, even at a concentration as low as 5%, for κa=6.56 (i.e., 10mM) the effect of finite concentration increases K to a value quite close to $1-\lambda$. Note that the concentration profiles indicate unambiguously that, whether solutes and pores are uncharged or of like charge, solute-solute interaction promotes enhanced concentrations near the pore wall. Consequently, the membrane rejection coefficients are estimated for different ionic strength of the solution. For illustration, Fig.6 displays the behavior of solute rejection for the case of infinitely dilute concentration.

The followings are pointed out as a concluding remarks. Due to the interplay of solute-solute and solute-wall interactions, the solute partition coefficient increases with the increase of solute concentration. Accordingly, the rejection coefficient of charged system is predicted to decrease with increasing solute concentration or ionic strength of solution, for a given value of relative pore size. Whereas the earlier methods fail to predict with increase of solute concentration, the present analysis can provide proper estimation within the context of charged system with non-dilute concentration.

Acknowledgement: Major part of this work was supported by NSF grant to Prof. R.J. Phillips and KOSEF fellowship for overseas study ('95-'96).

References

1. Belfort, G., R.H. Davis, and A.L. Zydney, "The behavior of suspensions and macromolecular solutions in crossflow microfiltration", *J. Membrane Sci.*, **96**, 1 (1994).
2. Bungay, P.M., H.K. Lonsdale, and M.N. de Pinho (eds.), *Synthetic Membranes: Science, Engineering and Applications*, pp.109-153, D. Reidel Pub., Dordrecht (1986).
3. Kaplan, F.S., T.B. Solomyak, and K.N. Brusov, "Ion-electrostatic interaction of microscopic objects of different geometry. Calculation of energy in a sphere-plane system", *Colloid J. of USSR*, **51**, 954 (1989).
4. Chun, M.-S., O.O. Park, and S.-M. Yang, "Concentration Depleted Layer due to Colloidal Force and its Influence on the Xanthan Fractionation", *J. Colloid Interface Sci.*, **161**, 247 (1993).

5. Seo, Y.H., O.O. Park, and M.-S. Chun, "The Behavior of Velocity Enhancement in Microcapillary Flows of Flexible Water-Soluble Polymers", *J. Chem. Eng. of Japan*, **29**, XXX (1996).
6. Deen, W.M., "Hindered Transport of Large Molecules in Liquid-Filled Pores", *AIChE J.*, **33**, 1409 (1987).
7. Phillips, R.J., W.M. Deen, and J.F. Brady, "Hindered Transport in Fibrous Membranes and Gels: Effect of Solute Size and Fiber Configuration", *J. Colloid Interface Sci.*, **139**, 363 (1990).
8. Chun, M.-S., and R.J. Phillips, "Electrostatic Partitioning in Slit-Pores by Gibbs Ensemble Monte Carlo Simulation", submitted manuscript.
9. Allen, M.P., and D.J. Tildesley, *Computer Simulation of Liquids*, Oxford Univ. Press, New York (1987).
10. Mitchell, B.D., and W.M. Deen, "Theoretical effects of macromolecule concentration and charge on membrane rejection coefficients", *J. Membrane Sci.*, **19**, 75 (1984).

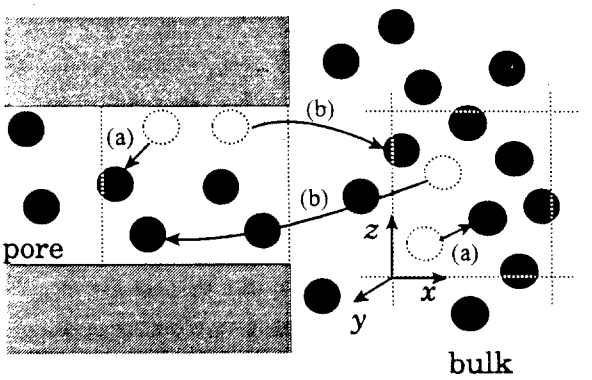

Fig.1. Illustration of the proposed GEMC method for simulation of equilibrium partitioning, dotted lines are periodic boundary conditions. (a) random particle displacement in each region, (b) particle interchange between two regions.

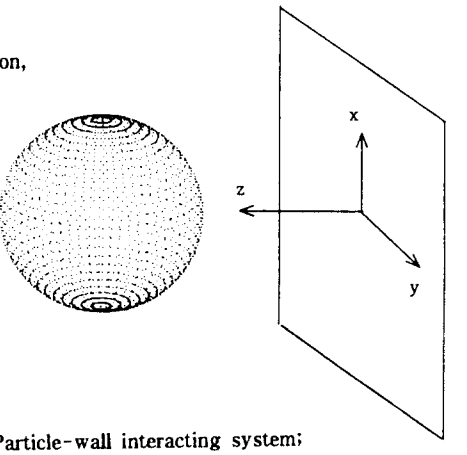

Fig.2. Particle-wall interacting system; surface points on the particle are spaced at $\pi/32$ rads in θ & ϕ directions.

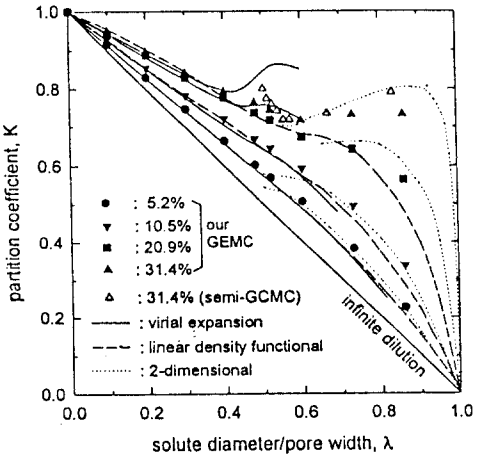

Fig.3. GEMC results for a purely steric partition coefficient with various solute concentrations. For comparison, previous results are provided; virial expansion (—), linear density functional (---), 2-dimensional approximation (·····), semi-grand ensemble MC simulations.

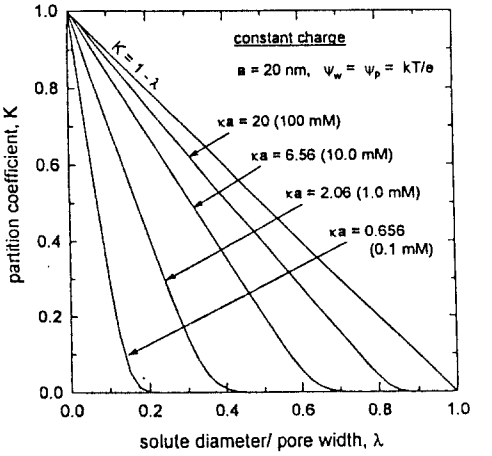

Fig.4. Partition coefficient with infinite dilute case, as a function of λ for several ionic strength of solution.

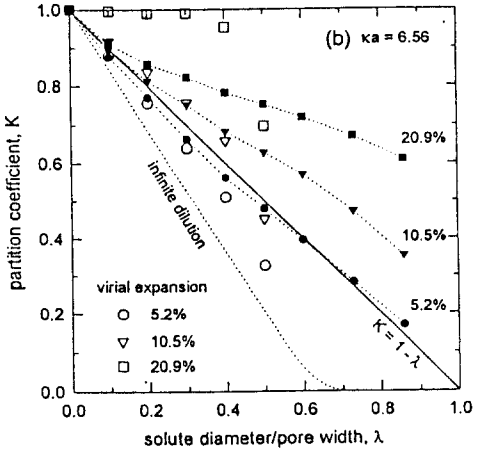

Fig.5. Partition coefficient with finite concentrated case, as a function of λ for ionic strength of 10mM. Virial expansion results are provided for the comparison.

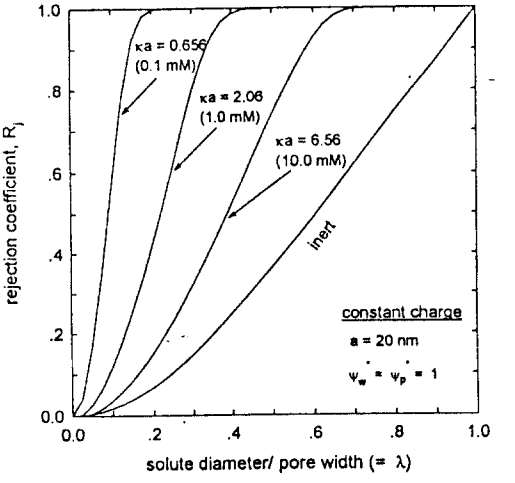

Fig.6. Rejection coefficient with infinite dilute case, as a function of λ for several ionic strength of solution.